# Structure-dependent ferromagnetism in $Au_4V$ studied under high pressure

D. D. Jackson,[1] J. R. Jeffries,[2] Wei Qiu,[3] Joel D. Griffith,[3] S. McCall,[1] C. Aracne,[1] M. Fluss,[1] M. B. Maple,[2] S. T. Weir,[1] and Y. K. Vohra[3]

[1]*Lawrence Livermore National Laboratory, Livermore, California 94551, USA*

[2]*Department of Physics and Institute for Pure and Applied Physical Sciences, University of California, San Diego, La Jolla, California 92093, USA*

[3]*Department of Physics, University of Alabama at Birmingham, Birmingham, Alabama 35124, USA*

(Received 2 August 2006; published 1 November 2006)

At ambient pressure, ordered $Au_4V$ is metallic and displays ferromagnetism at $T_C=45$ K. The electrical resistivity has been measured as a function of temperature from 1 K to 300 K and as a function of pressure up to 30 GPa using various high-pressure devices. A kink, which is associated with the reduction of scattering due to the onset of ferromagnetic order, is seen in the electrical resistance as a function of temperature. With applied pressure, this kink is found to broaden and increase in temperature at a rate of approximately 2.7 K/GPa. Above ~18 GPa, the broadening of the kink prohibits accurate determination of $T_C$; however, upon reducing the pressure, no signatures of ferromagnetism were evident in the electrical resistivity. Both energy-dispersive ($P \leq 61$ GPa) and angle-dispersive ($P \leq 27$ GPa) x-ray diffraction measurements at room temperature show a gradual transition from the body-centered-tetragonal phase of $Au_4V$ to a disordered face-centered-cubic structure. This transition is irreversible and continuous, and the data have been fit to a Birch-Murnaghan equation of state. In order to investigate the origin of the magnetic interactions in $Au_4V$, we have also measured the electrical resistivity of $Au_{1-x}V_x$ alloys and determined their Kondo temperatures $T_K$ for $x<1\%$. The pressure dependence of $T_K$ for $x=0.5\%$ was measured up to 2.8 GPa, for which the Kondo temperature increases at a rate of $dT_K/dP=6.5$ K/GPa. Using the volume dependence of the exchange interaction between magnetic vanadium ions, we find that the pressure-induced increase of the Curie temperature in $Au_4V$ can be explained by an increase in the exchange interaction parameter and the number of magnetic nearest neighbors.

DOI: 10.1103/PhysRevB.74.174401 PACS number(s): 72.10.Fk, 64.30.+t, 72.15.−v, 72.80.Ga

## I. INTRODUCTION

While both gold and vanadium are nonmagnetic metals, it was discovered in 1967 that, if annealed properly, the compound $Au_4V$ becomes ferromagnetic (FM) below $T_c \approx 43$ K.[1] The compound $Au_4V$ has a body-centered-tetragonal (bct) crystal structure with lattice constants of $a=6.3918\pm0.0053$ Å and $c=4.0392\pm0.0031$ Å. Figure 1(a) shows that the Au atoms form a distorted face-centered-cubic (fcc) lattice so that the unit cell volume of $Au_4V$ is roughly 2.5 times that of the unit cell volume of pure gold. Investigations into the origin of the FM phase were initially complicated due to the large magnetic anisotropy of the system, which resulted in disagreements as to the presence of a local moment. Creveling *et al.*[1] measured an effective moment of $1.43\mu_B$/f.u., indicative of a local moment with $s=1/2$, but the field-cooled saturation moment at 4.2 K was $M_{sat}=0.414\mu_B$/f.u., suggestive of an itinerant FM system. Luo and Creveling[2] investigated the specific heat of $Au_4V$ and found an anomaly near 50 K due to the onset of FM ordering, as expected for a local moment system. However, a large density of states was inferred from the electronic specific heat coefficient, which could have been consistent with an itinerant FM phase. Cohen *et al.*[3] performed Mössbauer measurements on Au-197 and inferred an effective moment on the vanadium ions of $0.92\mu_B$. Furthermore, they concluded that the effective field at the gold site was too small to be due to a polarization of the conduction electrons. The effective moment in the paramagnetic phase varied from sample to sample, and a second investigation by Creveling and Luo,[4] in which the magnetic susceptibility of over a dozen samples was measured, revealed that the majority of samples had an effective moment between $1.3\mu_B$/f.u., and $1.6\mu_B$/f.u., smaller than, but still consistent with, a spin-1/2 local moment on the vanadium site.

The low-temperature magnetic properties of $Au_4V$—which seemed to be consistent with itinerant ferromagnetism, largely as a result of the reduced saturation moment at 4.2 K—were difficult to investigate due to the very large coercive force. In the initial discovery of the FM behavior, no significant change in the magnetization was found at 4.2 K by increasing the field up to 1.1 T (Ref. 1); the saturation moment could only be determined by field cooling the sample. Subsequent measurements using a pulsed magnetic field revealed that the magnetization of $Au_4V$ saturated to a value of $1\mu_B$/f.u. at 29 T.[5] The accumulation of all of these results, both below and above the Curie temperature, provides strong evidence that the vanadium ions in $Au_4V$ carry a spin-1/2 local moment.

In ordered $Au_4V$, the vanadium nearest neighbors are all gold atoms, but in the disordered Au-20%V alloy, each vanadium ion has an average of 2.4 vanadium nearest neighbors. Claus *et al.*[6] speculated that in order for the vanadium ions to carry a local moment, their nearest neighbors must be predominantly Au ions. Furthermore, by measuring the properties of a Au-1%V alloy, they claim that another important parameter is the number of second nearest neighbors, for which it is essential that some of these be vanadium. Therefore, the V nearest and next-nearest neighbors are crucial in

 

determining whether or not the V ions develop a local moment. Cohen *et al.*[3] expanded on these ideas and postulated that the crystal field of $Au_4V$ is responsible for the existence of its local moment.

Induced strain has been shown to dramatically reduce the saturation moment at 1.5 K as well as to cause the crystal structure to transform from the body-centered-tetragonal structure of ordered $Au_4V$ to the face-centered-cubic structure of Au.[7] This drop in the saturation moment means that the signature of the FM phase will become more difficult to identify using a technique such as ac magnetometry at high pressure.[8] We have, therefore, identified the Curie temperature with a kink in the electrical resistivity $\rho(T)$ curve, where the kink is conveniently located by a peak in the second derivative of the $\rho(T)$ curve.[9] We have used three different methods under various degrees of hydrostatic conditions to investigate the electrical resistivity under pressure. In addition, we have used x-ray diffraction measurements up to 61 GPa in order to investigate the transition from ordered $Au_4V$ to a disordered Au-20% V alloy. Finally, in order to gain insight into the origin of the magnetic interactions, we have investigated the electrical resistivity of Au with low V concentrations in order to characterize the Kondo behavior as a function of concentration and pressure. Because the Kondo contribution to the electrical resistivity does not change appreciably with V concentration, we measured the pressure dependence of Au-0.5% V in order to determine the change in the magnetic interaction with increasing pressure.

## II. EXPERIMENTAL TECHNIQUES

Preparation of the arc-melted and annealed $Au_4V$ sample used for this work has been described elsewhere (Creveling and Luo,[4] sample No. 3). The magnetization of the sample has been remeasured using a commercial Quantum Design MPMS superconducting quantum interference device (SQUID) magnetometer.

Polycrystals of $Au_{1-x}V_x$—also denoted as Au-$x$% V, where $x$ is the vanadium concentration in atomic percent—with nominal vanadium concentrations $x$=10%, 5%, 2%, 1%, 0.50%, 0.25%, 0.20%, and 0.10% were synthesized using conventional arc-melting techniques. The vanadium pieces (Johnson Matthey Chemicals, SpecPure, Lab No. 551229) were first etched in a 10% $HNO_3$:$H_2O$ solution to remove any oxide layer. Both the gold (Colonial Metals, 99.99%, Lot No. 2000-R4691-1) and the etched vanadium pieces were then placed in acetone and cleaned in an ultrasonic cleaner for 30 min. The gold and vanadium were then weighed and combined stoichiometrically to produce an approximately 3-g "master alloy" of Au-10% V to be used in the synthesis of the compounds with smaller values of $x$. After weighing, the constituent materials were placed in an arc furnace and arc-melted several times using arc currents from 50 to 200 A, flipping the boule between successive melts. Small slices were then taken from the "master alloy" and combined and arc-melted as above with the appropriate amount of gold necessary to produce approximately 1 g masses each of the other Au-$x$% V samples with nominal vanadium concentrations $x$=5%, 2%, 1%, 0.50%, and 0.25%. The very low vanadium concentration samples of $x$ =0.20% and 0.10% were made as above using small pieces from the 1%, as opposed to the 10%, sample as their "master alloy." Weight losses were less than 0.1% for all samples.

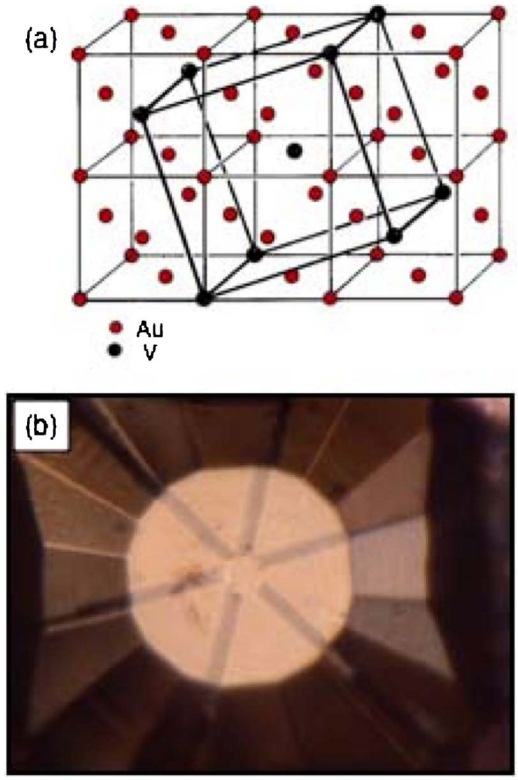


FIG. 1. (Color online) (a) The crystal structure of $Au_4V$ showing both the bct ordered structure and the distorted fcc arrangement of Au (Ref. 24). (b) The designer diamond used for this work. A standard four-probe technique was used, leaving two extra leads for redundancy.

Three types of pressure cells were used in this study: a clamped piston-cylinder cell, a Bridgman anvil cell, and a diamond anvil cell (DAC). Each technique had some overlap in pressure, and the differences in the location of the Curie temperature between each method were negligible. For nearly hydrostatic pressures below 3 GPa, a clamped piston-cylinder cell was used. The sample, which had four electrical leads (2 mil diameter gold wire) attached using EpoTek H20E silver epoxy, was loaded along with a Pb manometer into a Teflon capsule filled with Fluorinert FC75 as the pressure-transmitting medium. The pressure inside the capsule was determined inductively from the pressure-dependent superconducting transition of a Pb manometer.[10]

Pressures up to 5 GPa were produced using a Bridgman anvil technique.[11] The Bridgman anvil cell was comprised of two opposed tungsten carbide anvils that compressed the sample chamber, which consisted of a pyrophyllite gasket with an inner diameter of 2.0 mm and two steatite disks that served as the pressure-transmitting medium. The sample was cut and polished to approximate dimensions $500\times220\times45$ $\mu m^3$ and then placed between the two steatite disks in electrical contact with a small piece of lead of similar dimensions. Six platinum wires (2 mil diameter) were

inserted through the pyrophyllite gasket with three wires placed in contact with the sample and the other three wires placed in contact with the Pb manometer. The resistive superconducting transition of the Pb manometer was used with the pressure scale of Bireckoven and Wittig[12] to determine the pressure inside of the sample chamber. For both the clamped piston-cylinder and Bridgman anvil cells, four-probe ac electrical resistance measurements from 1 K to 300 K were made in a $^4$He cryostat using a Linear Research LR-201 ac resistance bridge with a frequency of 16 Hz and excitation currents of 1–10 mA.

A designer diamond anvil, as seen in Fig. 1(b), was used for a standard four-probe electrical resistivity measurement for pressures up to 30 GPa. This is a specially prepared diamond that consists of a standard 1/3 carat brilliant cut diamond anvil with a set of tungsten thin film probes patterned on its surface using three-dimensional (3D) laser pantography and 2D projection lithography, followed by high-quality epitaxial diamond chemical vapor deposition (CVD).[13] Designer diamond anvil technology has been used for both electrical resistivity[13,14] and ac magnetic susceptibility measurements.[8] Typical probe line widths are 5–10 $\mu$m and probe thicknesses range from 0.2 to 0.7 $\mu$m. These line patterns extend from the 300-$\mu$m-diam culet of the anvil, where the high-pressure sample is located, down the side of the anvil to 125 $\mu$m$\times$250 $\mu$m pads that serve as connection points for external instrumentation. Error in the resistance was typically less than 0.3%. The temperature-dependent electrical resistance was measured using a closed-cycle He cryostat (CryoMech ST15) and a DAC (manufactured by Kyowa Seisakusho Co., screw type) with no pressure medium. A small ruby chip was also placed in the gasket hole with the sample and used as a pressure marker. The pressure was measured at room temperature using the standard ruby scale.[15] Delrin washers of suitable thickness were added to the DAC piston to overcome changes in the pressure due to thermal contraction of the cell. Due to these changes and pressure gradients, the uncertainty in pressure was estimated to be 5%.

The high-pressure structural experiments were performed in a DAC with a culet diameter of 300 $\mu$m. A piece of $Au_4V$ sample was loaded in the 80-$\mu$m sample chamber along with the ruby pressure marker; no hydrostatic medium was used. Two sets of x-ray diffraction experiments were carried out to investigate the crystalline phases and their compressibility. The first experiment utilized an energy dispersive x-ray diffraction (EDXD) technique up to pressures of 61 GPa. The second experiment utilized an angle-dispersive x-ray diffraction (ADXD) technique to a highest pressure of 27 GPa. The EDXD spectra were recorded at the superconducting wiggler beamline X-17C at the National Synchrotron Light Source, Brookhaven National Laboratory. The ADXD spectra were recorded at the sector 16-ID-B beamline at the Advanced Photon Source, Argonne National Laboratory. In both diffraction experiments, the collimated x-ray beam size was around 11 $\mu$m$\times$15 $\mu$m. The pressure inside the chamber was determined as in the electrical resistivity measurements above.

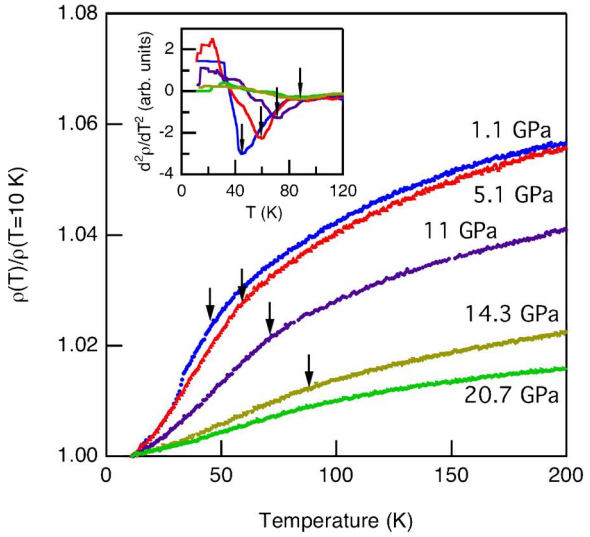


FIG. 2. (Color online) $\rho(T)$ normalized at 10 K as a function of temperature for 1.1, 5.1, 11.0, 14.3, and 20.7 GPa, all collected using a designer diamond in a DAC. The inset shows $d^2\rho/dT^2$ as a function of temperature $T$ in which the peak was used to locate the Curie temperature, denoted by the downward arrows.

## III. RESULTS

### A. Electrical resistivity of $Au_4V$

An analysis of the magnetization of the sample using a commercial SQUID magnetometer gives $T_c$=45 K and an effective magnetic moment in the paramagnetic phase of $p_{eff}$=1.53$\mu_B$/f.u., which is in good agreement with the published results,[4] showing no degradation in sample quality. Figure 2 shows $\rho(T)/\rho(T=10\ \mathrm{K})$ for typical measurements using the DAC. The results using both the piston-cylinder and Bridgman anvil cells looked similar, with the latter having a larger residual resistivity ratio (RRR) due to the presence of a quasihydrostatic pressure medium. The location of the Curie temperature was determined by the location of the negative peak in $d^2\rho/dT^2$ (inset to Fig. 2). For $P \lesssim 18$ GPa, the Curie temperature increased linearly with pressure at a rate of $dT_C/dP$=2.7 K/GPa [Fig. 6(b), below]. In this pressure range, the height of the peak of $d^2\rho/dT^2$ decreased monotonically with pressure, while for $P \gtrsim 18$ GPa, the height of the peak remained roughly constant and at a value too small to allow an accurate determination of a transition temperature [Fig. 6(c), below]. The $\rho(T)$ curves in Fig. 2 show that the RRR decreases as the pressure increases; a sharp drop occurs near 18 GPa, followed by a flattening of the *RRR* [Fig. 6(d), below]. The electrical resistivity was also measured as the pressure was reduced, and the resulting curves remained within 0.15% of each other, showing no clear signature of magnetic ordering (data not shown for clarity).

### B. X-ray diffraction measurements on $Au_4V$

The image plate of the ADXD data for different pressures shows the disappearance of tetragonal diffraction peaks (110), (101), and (200) at 27 GPa. Upon decompression of

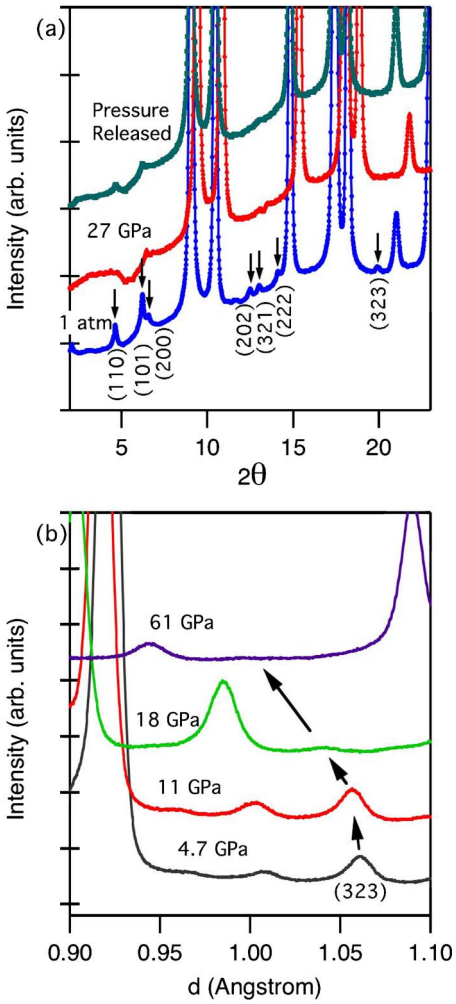


FIG. 3. (Color online) (a) Angle-dispersive x-ray diffraction (ADXD) spectra after the integration of the 2D image plates. The (*hkl*) diffraction peaks characteristic of the tetragonal phase become very weak as pressure increases and do not reappear after downloading the pressure. (b) Energy-dispersive x-ray diffraction (EDXD) spectra of the $Au_4V$ sample under different pressures up to 61 GPa. The (323) diffraction peak associated with the tetragonal phase is suppressed with applied pressure, becoming indistinguishable above 18 GPa.

the DAC, the aforementioned tetragonal diffraction peaks remained absent. The spectra of 2D integration of image plates in Fig. 3(a) clearly show the disappearance of more tetragonal diffraction peaks: (202), (321), (222), and (323). Calculations indicate the phase transformation of the $Au_4V$ sample from the initial tetragonal phase at ambient pressure, with $a=6.3918\pm0.0053$ Å and $c=4.0392\pm0.0031$ Å, to a disordered fcc phase, with $a=3.8937\pm0.0015$ Å at 27 GPa. After decompression, the $Au_4V$ sample remained in the disordered fcc phase with $a=4.0244\pm0.0020$ Å. The results of the ADXD experiment seem to indicate that the high-pressure phase transformation in $Au_4V$ is gradual in nature. Under the highest pressure of 27 GPa, we can say the phase transformation is almost complete.

The second EDXD experiment of the same $Au_4V$ sample to 61 GPa helped us extend the pressure range and verify our conclusion of the phase transformation. Upon increasing pressure, all strong diffraction peaks shifted to higher energies, indicative of a compression of the interplanar spacing of the lattice. However, Fig. 3(b) clearly shows the suppression of peak (323), which is a typical tetragonal phase diffraction peak, with applied pressure. We found that the initial (323) peak became too weak to be identified for pressures in excess of 18 GPa. For pressures in excess of 18 GPa, the observed diffraction peaks from the $Au_4V$ sample can be assigned to a disordered cubic fcc phase. The disordered fcc phase persisted to the highest attained pressure of 61 GPa, where $a=3.7762\pm0.0020$ Å. As before, the sample remained in the disordered fcc phase after decompression.

Finally, we can combine all our x-ray diffraction data to evaluate the compressibility of the $Au_4V$ sample. The inset of Fig. 6(a), below, shows all pressure-volume data points from the x-ray diffraction data. The Birch-Murnaghan equation of state (EOS) of the third order,

$$P=\frac{3}{2}B_0\left[\left(\frac{V}{V_0}\right)^{-7/3}-\left(\frac{V}{V_0}\right)^{-5/3}\right]\times\left\{1+\frac{3}{4}\left(B_0'-4\right)\left[\left(\frac{V}{V_0}\right)^{-2/3}-1\right]\right\}, \quad (1)$$

where $B_0$ is the bulk modulus and $B_0'$ is the first derivative of bulk modulus,[23] was used to fit our *P-V* data for the pressure range between 1 atm (0.1 MPa) and 61 GPa. This EOS exhibited a good fit to the measured compression of the $Au_4V$ sample to 61 GPa as shown in Fig. 6(a), below. The EOS parameters $B_0=207.11\pm2.32$ GPa and $B_0'=3.62\pm0.12$ were obtained for $V_0=16.5023$ Å$^3$, where $V_0$ represents the volume per atom.

### C. Electrical resistivity of $Au_{1-x}V_x$

Due to the increase in the Curie temperature as a function of pressure in $Au_4V$, samples of $Au_{1-x}V_x$ with various vanadium concentrations ($x=0.10\%$, 0.20%, 0.25%, 0.50%, 1%, 2%, 5%, and 10%) were synthesized and characterized via electrical resistivity in order to examine the effect of pressure on the Kondo interactions present in this dilute alloy. Specimens of $Au_{1-x}V_x$ with $x<1\%$ exhibited the Kondo effect, observable as a minimum in the electrical resistivity as a function of temperature, consistent with previous measurements by Kume.[16] The position of this minimum $T_{min}$ as a function of vanadium concentration $x$ is consistent with the $x^{1/3}$ dependence obtained from Kondo's theory of the resistance minimum when the electrical resistivity of the host metal (in this case, Au) varies as $T^3$.[17] A sample of Au-0.5%V was chosen for high-pressure studies due to the presence of the deep Kondo minimum.

Figure 4 shows the electrical resistivity as a function of temperature at various pressures for a sample of Au-0.5%V. The characteristic Kondo minimum can be seen at $T_{min}\approx20$ K at ambient pressure, evolving very little with applied pressure. The value of the residual resistivity increases by approximately 7% from ambient pressure up to 2.8 GPa. The magnetic component of the electrical resistivity, $\Delta\rho_M(T)$, was calculated as the measured

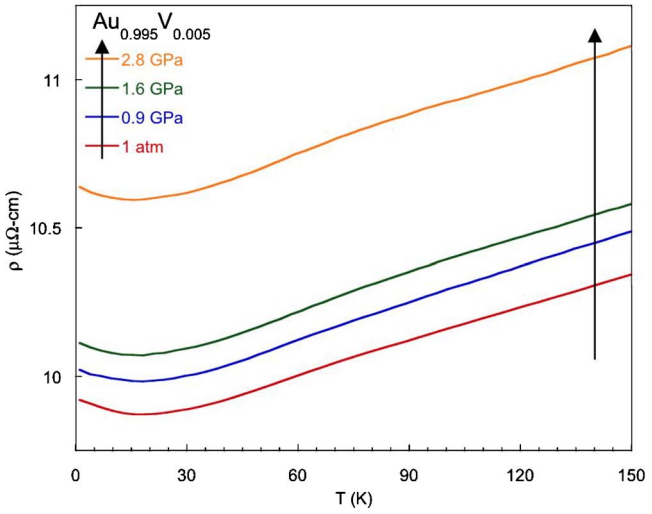


FIG. 4. (Color online) The electrical resistivity as a function of temperature for Au-0.5% V for various pressures. The minimum in the electrical resistivity at $T_{min} \approx 20$ K for the ambient pressure curve is a hallmark of the Kondo effect. With applied pressure, $T_{min}$ is only slightly affected; however, the residual resistivity increases by approximately 7% from ambient pressure to 2.8 GPa.

electrical resistivity minus that of pure gold [i.e., $\Delta\rho_M(T) = \rho_{meas}(T) - \rho_{Au}(T)$].

The Kondo temperature $T_K$ as a function of pressure was extracted from the normalized magnetic component of the electrical resistivity $\Delta\rho_M(T)/\Delta\rho_M(0)$ as seen in Fig. 5, with $T_K$ defined, following the method of Seaman and Maple, as the temperature at which $\Delta\rho_M(T)/\Delta\rho_M(0) = 0.8$.[18] The ambient pressure value of $T_K \approx 182$ K obtained from this method is significantly lower than previously reported values, which were defined in a different manner.[19] It was found that plots of $\Delta\rho_M(T)/\Delta\rho_M(0)$ as a function of $T/T_K$ (not shown) for the various pressures scaled such that the curves lied on top of one another, indicating an accurate determination for $T_K$. The inset of Fig. 5 displays $T_K$ increasing as a function of pressure at a rate of approximately 6.5 K/GPa; the increase in $T_K$ with pressure is consistent with that expected of a negative exchange interaction associated with the Kondo effect.[19–21]

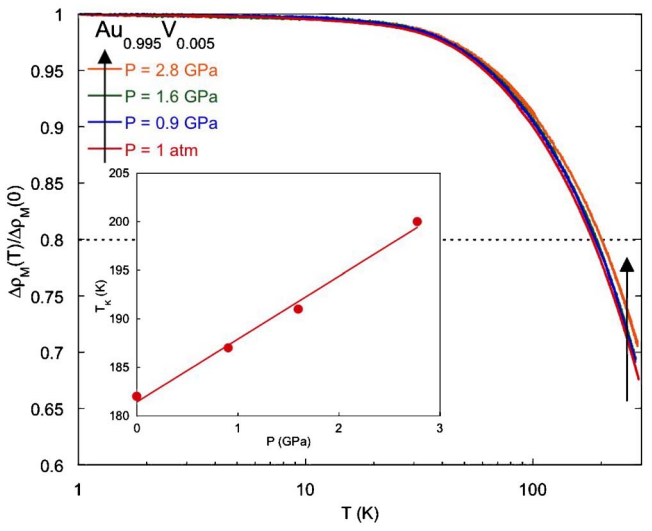


FIG. 5. (Color online) A semilogarithmic plot of the normalized magnetic component of the electrical resistivity $\Delta\rho_M(T)/\Delta\rho_M(0)$ (defined in the text) as a function of temperature for various pressures shows the evolution of the Kondo temperature $T_K$ for Au-0.5% V. The Kondo temperature is defined as the temperature at which $\Delta\rho_M(T)/\Delta\rho_M(0) = 0.8$ (horizontal dashed line), corresponding to a deviation from the higher temperature behavior. The inset shows $T_K$ as determined from the above criteria as a function of pressure; the line is a linear fit to the data.

## IV. DISCUSSION

By investigating the increase of the Curie temperature with three different techniques, we were able to look for differences between the results with (piston-cylinder cell and Bridgman anvil cell) and without (DAC) a quasihydrostatic medium. While the RRR was larger when measured with a nearly hydrostatic medium (RRR=1.59 at 0.1 GPa) compared with the DAC (RRR=1.06 at 1.1 GPa), the pressure derivative of the Curie temperature was identical within experimental error. The DAC, therefore, can confidently be used to investigate the behavior for $P > 5$ GPa. Furthermore, we have used the same configuration for the structural analysis in order to obtain a consistent picture of the behavior of the material up to the highest pressures.

A change in behavior of the electrical resistivity occurs at approximately 18 GPa. This can be clearly seen in Fig. 6, where the leftmost vertical black line indicates $P^* \simeq 18$ GPa for all plots. First, the pressure dependence of $T_C$ above $P^*$ seems to deviate from the linear fit below $P^*$ [Fig. 6(b)]. Furthermore, with increasing pressure, the height of the peak in $d^2\rho/dT^2$ monotonically decreases towards zero near $P^*$; pressures in excess of $P^*$ reveal a relatively pressure-independent and very small value of the peak in $d^2\rho/dT^2$ [Fig. 6(c)]. While the Curie temperature is typically located to within 3 K below $P^*$, at higher pressures, the uncertainty more than doubles and it becomes difficult to convincingly show that a ferromagnetic phase persists. Finally, the value of the RRR is seen to monotonically decrease in a similar fashion to the height of the peak in $d^2\rho/dT^2$ up to $P^*$ [Fig. 6(d)], after which the RRR remains roughly constant, signifying a change in the scattering mechanism due to the suppression of ferromagnetism as well as a change in the crystalline structure in this pressure region. All of the above qualitative changes suggest that $Au_4V$ undergoes a gradual pressure-induced phase transition from an ordered ferromagnetic state to a state showing no magnetic order above $P^*$. Zero-field-cooled and field-cooled magnetization measurements of the sample (still within the gasket) after decompression showed no discernible differences, suggesting that ferromagnetic behavior is not recovered upon decompression. It should be noted that the estimated magnitude of a ferromagnetic signal from the sample inside the gasket would have been less than one order of magnitude greater than the minimum sensitivity of the magnetometer used. The fact that no signature of magnetic ordering was recovered on downloading the pressure cell indicates that the phase transition at $P^*$ is irreversible.

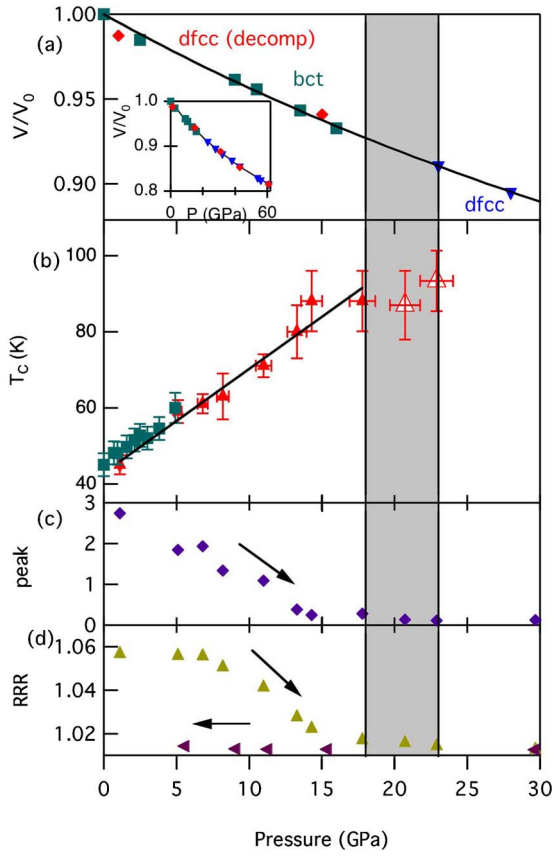


FIG. 6. (Color online) (a) The measured equation of state of $Au_4V$ up to 30 GPa at 300 K (inset shows data up to 61 GPa) obtained from the x-ray diffraction experiments. The square symbols represent the low-pressure tetragonal phase, the triangle symbols represent the disordered fcc phase for pressure above 18 GPa, the diamond symbols represent the disordered fcc phase of the decompressed $Au_4V$ sample, and the solid curve is the fit to the Birch-Murnaghan third-order equation of state (1). (b) $T_C$ with the squares from the piston-cylinder and Bridgman cells and the triangles from the DAC. The two highest-pressure data points are differentiated by open triangles due to the significantly higher uncertainty in assigning a transition temperature at these pressures. (c) The height of the peak observed in $d^2\rho/dT^2$. (d) RRR defined as $\rho(T=200\ \mathrm{K})/\rho(T=10\ \mathrm{K})$, with the upward-pointing triangles indicating increasing pressure in the DAC and the leftward-pointing triangles indicating decreasing (downloading) pressure in the DAC. The shaded area bordered by vertical black lines indicates the region of the broad phase transition; the low- and high-pressure boundaries are determined from EDXD and ADXD measurements, respectively.

In addition to the loss of a definitive signature of magnetism, a gradual structural phase transition occurs near $P^*$, which is complete by $P=27$ GPa and is nonreversable when downloading the pressure. Both the slow decrease in the signature for the Curie temperature and the slow disappearance of the tetragonal x-ray peaks without a volume change suggest that $Au_4V$ undergoes a gradual phase transition from the ordered bct structure to the disordered fcc structure of the Au-20%V alloy. It should be noted that the breadth in pressure of this phase transition could have been exacerbated by the lack of an additional hydrostatic pressure medium inside the sample chamber of the DAC's, which may have produced pressure gradients upon the sample. Regardless, this structural phase change is consistent with the disappearance of magnetic ordering inferred from the electrical resistivity, as the disordered fcc structure of the Au-20%V alloy has been shown to be nonmagnetic.[4] Furthermore, upon downloading the pressure of both the electrical resistivity and x-ray diffraction cells, no evidence for magnetic ordering or a transition into the tetragonal crystal structure was observed, illustrating the implicit relation between structure and magnetism in $Au_4V$.

Previous measurements of the dilute Au-V alloy system suggest that these alloys retain a local moment on the V site up to $x \simeq 30\%$ (the disordered alloy from which ordered $Au_4V$ forms upon annealing is Au-20%V), above which a Curie tail is not observed in the magnetic susceptibility.[4] The observation of the resistivity minimum in the Au-0.5%V alloy measured under pressure in this study arises from the Kondo effect, which requires the presence of local moments and has a characteristic temperature

$$T_K \simeq T_F e^{[-1/|JN(E_F)|]}, \tag{2}$$

where $T_K$ is the Kondo temperature, $T_F$ is the Fermi temperature, $J$ is the exchange interaction parameter characterizing the interaction between the local moments and the conduction electron spins, and $N(E_F)$ is the density of states at the Fermi level.[22,23] As pressure is applied to the system, the volume decreases and the ions move closer together, which decreases $N(E_F)$ and increases $|J|$. For a simple free electron gas, $T_F$ is proportional to $1/N(E_F)$ and $N(E_F) \propto V^{2/3}$, such that $d \ln N(E_F)/d \ln V = 0.67$. We can then use our measured values for the pressure dependence of the Kondo temperature, $d \ln T_K/dP$, and the EOS determined from the Birch-Murnaghan fit to the x-ray data, $d \ln V/dP$, to estimate the change in the exchange interaction parameter with volume, $d \ln|J|/d \ln V$. We find that the Kondo temperature increases with decreasing volume as $d \ln T_K/d \ln V \approx -7$. This value compares reasonably well to the value reported by Schilling of $d \ln T_K/d \ln V = -17$,[19] with discrepancies due to factors such as sample dependence, determination of $T_K$, or disparities in compressibility data. This observed increase in the Kondo temperature of Au-0.5%V with pressure is dominated by an increase in the magnitude of the exchange interaction parameter $|J|$ with decreasing volume, $d \ln|J|/d \ln V = -1.8$, about half the value reported by Schilling, but more representative of other transition-metal Kondo systems.[19]

The results of magnetization[5] and Mössbauer[3] measurements in conjunction with the aforementioned presence of local moments in the disordered Au-20%V alloy favor a local moment scenario for the magnetism of $Au_4V$; however, the exchange mechanism for the FM ordering is not understood. A possible mechanism responsible for the ferromagnetism in $Au_4V$ is the RKKY interaction, in which the interatomic exchange is mediated via the exchange interaction between the local moments and the conduction electron spins.[22] In the RKKY picture, the ordering temperature $T_{RKKY}$ is proportional to both the density of states $N(E_F)$ and the square of the exchange interaction parameter,

$T_{RKKY} \propto N(E_F)J^2$. Thus, $d \ln T_{RKKY}/d \ln V = 2d \ln|J|/d \ln V + d \ln N(E_F)/d \ln V$, which, using the measured rate of change of $J$ for Au-0.5%V and a free electron value for $d \ln N(E_F)/d \ln V = 0.67$, yields an expected value $d \ln T_{RKKY}/d \ln V \approx -4.5$. However, the Curie temperature was found to increase at a rate about twice this, $d \ln T_C/d \ln V = -9.9$. Given the uncertainties in estimating the pressure dependence of $T_K$, the differences in structure and compressibility between the Au-0.5%V alloy and the compound $Au_4V$, and the use of a free electron model, the discrepancy between the measured pressure dependence of $T_C$ in $Au_4V$ and the expected pressure dependence of $T_{RKKY}$ is not unreasonable and does not rule out the RKKY interaction as the mechanism for the FM ordering in $Au_4V$.

As another approach, we consider a mean-field approximation including only nearest-neighbor interactions to examine the behavior of the Curie temperature within the context of a Heisenberg-type exchange interaction:

$$T_C = \frac{2zS(S+1)\mathcal{J}}{3k_B}, \tag{3}$$

where $z$ is the number of magnetic nearest neighbors, $S$ is the spin of the vanadium ions, $k_B$ is Boltzmann's constant, and $\mathcal{J}$ is the interatomic exchange interaction parameter. Thus, using Eq. (3), the volume dependence of $T_C$ can be estimated from the volume dependence of $\mathcal{J}$, which is proportional to $N(E_F)J^2$ in an RKKY scenario, yielding the same result as found above for $d \ln T_{RKKY}/d \ln V$. While the sign of $d \ln T_C/d \ln V$ is consistent with the sign of $d \ln \mathcal{J}/d \ln V$, its magnitude is about 2 times as large as expected from the magnitude of $d \ln \mathcal{J}/d \ln V$ (or equivalently $d \ln[N(E_F)J^2]/d \ln V$). Therefore, we consider the changes in the number and separation of V-V nearest neighbors as the $Au_4V$ volume decreases and the structure gradually changes under pressure and explore the possible consequences.

It has been suggested that the number of V-V nearest neighbors and their separation from each other plays a substantial role in the magnetic properties such as the effective moment and the presence of magnetic ordering in $Au_4V$.[3,4,6] In the disordered Au-20%V alloy, each V has, on average, $12 \times 0.2$ nearest neighbors within a radius of $(\sqrt{2}/2)a$, and $6 \times 0.2$ second-nearest neighbors within $a$, for a total of 3.6 vanadium neighbors within a sphere of radius equal to the lattice spacing of one unit cell. As can be seen from Fig. 1, the number of V-V nearest neighbors in the ordered $Au_4V$ lattice is greatly reduced, as their are only two V-V nearest neighbors within a radius $a$, a distance equivalent to the cubic unit cell length of the fcc lattice. Our structural analysis shows that the transition from the ordered bct structure of $Au_4V$ to the disordered fcc structure of Au-20%V is very gradual. It is reasonable to assume that the number of V-V nearest neighbors will also gradually change during this transformation as the V ions become randomly positioned within the fcc lattice. We can therefore use Eq. (3) in combination with the value of $d \ln|J|/d \ln V$ obtained from experiment to estimate the volume dependence of the V-V nearest neighbors to be $d \ln z/d \ln V = -7.0$. Using this value and Eq. (1), the pressure at which the number of V-V nearest neighbors increases from 2 to 3.6 is approximately 21 GPa, a value which lies within the shaded region of Fig. 6 that indicates the location of the gradual phase transition inferred from x-ray diffraction and electrical resistivity data.

In the framework of our results, a decrease in volume causes the magnetic coupling between V ions to increase, as was found by the increase in the Kondo temperature in Au-0.5%V. This increase in the magnetic exchange parameter for $Au_4V$ is also accompanied by a gradual transformation to the Au-20%V alloy, which results in an increase in the number of V-V nearest neighbors. The combination of the two effects results in a large increase in the Curie temperature. Near $P^*$, however, the number of V-V nearest neighbors increases by approximately 60%, according to our results, and this increase is sufficient to, on average, suppress FM ordering, resulting in a small and subtle signature for the magnetic transition in the resistivity. As the pressure is increased toward 28 GPa, the V ions become increasingly randomly dispersed throughout the Au sites, which manifests itself as a significant weakening in the tetragonal peaks in the x-ray diffraction pattern. It should be noted that Cohen *et al.* postulated that the crystalline electric field (CEF) differences between the ordered $Au_4V$ and disordered Au-20%V were responsible for the large difference between effective magnetic moments in the two crystal structures;[3] however, no CEF analysis was performed in this work. This postulate of a pressure-induced increase in the number of V-V nearest neighbors is, thus, only one of many plausible explanations, and without adequate electronic structure calculations for either the ordered $Au_4V$ or the disordered Au-20%V alloy, it is impossible to identify the driving mechanism for FM ordering, its increase with pressure, and its eventual destruction at high pressure in $Au_4V$.

## V. CONCLUSION

Under ambient conditions, the $Au_4V$ sample studied in this work becomes FM at $T_C = 45$ K. Applying pressure to this ordered phase results in an increase of the Curie temperature at a rate of $dT_C/dP = 2.7$ K/GPa. In addition, alloys of Au with low concentrations of V show the Kondo effect, with pressure measurements on an alloy of Au-0.5%V revealing an increase of the Kondo temperature of $dT_K/dP = 6.5$ K/GPa. While the sign of $d \ln T_C/d \ln V$ is consistent with that of $d \ln \mathcal{J} \ln V$, its magnitude is about twice as large as estimated from an RKKY mechanism alone. The discrepancy may be related to changes in the number and separation of V-V nearest neighbors with pressure. X-ray diffraction measurements of $Au_4V$ up to 61 GPa reveal a gradual and continuous structural phase transition from the bct structure of $Au_4V$ to the fcc structure of the Au-20%V alloy between 18 and 23 GPa. A loss of the signature in electrical resistivity associated with the onset of ferromagnetic order occurs at $P^* \simeq 18$ GPa. The gradual transformation to the disordered fcc structure is most likely responsible for the destruction of magnetic ordering by altering the number of V-ion nearest neighbors.

**ACKNOWLEDGMENTS**

We would like to thank Dave Ruddle and Steve Falabella for their help in the experiments. We also thank L. T. Wiley, B. T. Goodwin, and J. Akella for their support of this work. Work at LLNL was performed under the auspices of the U.S. Department of Energy by the University of California, Lawrence Livermore National Laboratory, under Contract No. W-7405-Eng-48. Research at UCSD was sponsored by the U.S. Department of Energy under Grant No. DE-FG02-04ER46105, the U.S. National Science Foundation under Grant No. DMR-0335173, and the National Nuclear Security Administration under the Stewardship Science Academic Alliances program through DOE Research Grant No. DE-FG52-03NA00068. The UAB research team would like to acknowledge support from the Department of Energy (DOE) under Grant No. DE-FG52-06NA26168.

[1] L. Creveling, H. L. Luo, and G. S. Knapp, Phys. Rev. Lett. **18**, 851 (1967).
[2] H. L. Luo and L. Creveling, Phys. Lett. **25A**, 740 (1967).
[3] R. Cohen, J. Wernick, K. W. West, R. Sherwood, and G. Y. Chin, Phys. Rev. **188**, 684 (1969).
[4] J. L. Creveling and H. Luo, Phys. Rev. **176**, 614 (1968).
[5] G. Kido and N. Miura, J. Magn. Magn. Mater. **31-34**, 283 (1983).
[6] H. Claus, A. K. Sinha, and P. A. Beck, Phys. Lett. **26A**, 38 (1967).
[7] G. Y. Chin, J. H. Wernick, R. C. Sherwood, and D. R. Mendorf, Solid State Commun. **6**, 153 (1968).
[8] D. Jackson, C. Aracne-Ruddle, V. Malba, S. Weir, S. Catledge, and Y. Vohra, Rev. Sci. Instrum. **74**, 2467 (2003); D. D. Jackson, V. Malba, S. T. Weir, P. A. Baker, and Y. K. Vohra, Phys. Rev. B **71**, 184416 (2005).
[9] M. B. Maple and H. Luo, Phys. Lett. **25A**, 121 (1967).
[10] T. F. Smith, C. W. Chu, and M. B. Maple, Cryogenics **54**, 53 (1969).
[11] J. Wittig, Z. Phys. **195**, 215 (1966).
[12] B. Bireckoven and J. Wittig, J. Phys. C **21**, 841 (1988).
[13] S. Weir, J. Akella, C. Aracne-Ruddle, Y. Vohra, and S. A. Catledge, Appl. Phys. Lett. **77**, 3400 (2000).
[14] N. Velisavljevic, Y. Vohra, and S. Weir, High Press. Res. **25A**, 137 (2005); N. Velisavljevic, K. MacMinn, Y. Vohra, and S. Weir, Appl. Phys. Lett. **84**, 927 (2004); J. R. Patterson, S. A. Catledge, Y. K. Vohra, J. Akella, and S. T. Weir, Phys. Rev. Lett. **85**, 5364 (2000).
[15] J. D. Barnett, S. Block, and G. J. Piermarini, Rev. Sci. Instrum. **44**, 1 (1973); H. Mao, P. Bell, J. W. Shaner, and D. Steinberg, J. Appl. Phys. **49**, 3276 (1978); D. Ragan, R. Gustavsen, and D. Schiferl, *ibid.* **72**, 5539 (1992).
[16] K. Kume, J. Phys. Soc. Jpn. **22**, 1116 (1967).
[17] J. Kondo, Prog. Theor. Phys. **32**, 37 (1964).
[18] C. L. Seaman and M. B. Maple, Physica B **199&200**, 396 (1994).
[19] J. S. Schilling, Adv. Phys. **28**, 657 (1979).
[20] K. S. Kim and M. B. Maple, Phys. Rev. B **2**, 4696 (1970).
[21] M. B. Maple and J. Wittig, Solid State Commun. **9**, 1611 (1971).
[22] A. C. Hewson, *The Kondo Problem to Heavy Fermions*, Cambridge Studies in Magnetism Vol. 2 (Cambridge University Press, Cambridge, England, 1993).
[23] *High Velocity Impact Phenomenon*, edited by R. Kinslow (Academic, New York, 1970).
[24] J. Kubler, J. Magn. Magn. Mater. **45**, 415 (1984).